

Game-theoretic Objective Space Planning

Hongrui Zheng, Zhijun Zhuang, Johannes Betz, Rahul Mangharam

Abstract—Autonomous Racing awards agents that react to opponents’ behaviors with agile maneuvers towards progressing along the track while penalizing both over-aggressive and over-conservative agents. Understanding the intent of other agents is crucial to deploying autonomous systems in adversarial multi-agent environments. Current approaches either oversimplify the discretization of the action space of agents or fail to recognize the long-term effect of actions and become myopic. Our work focuses on addressing these two challenges. First, we propose a novel dimension reduction method that encapsulates diverse agent behaviors while conserving the continuity of agent actions. Second, we formulate the two-agent racing game as a regret minimization problem and provide a solution for tractable counterfactual regret minimization with a regret prediction model. Finally, we validate our findings experimentally on scaled autonomous vehicles. We demonstrate that using the proposed game-theoretic planner using agent characterization with the objective space significantly improves the win rate against different opponents, and the improvement is transferable to unseen opponents in an unseen environment.

I. INTRODUCTION

Highly interactive, multi-agent, competitive scenarios remain the center of Autonomous Vehicle (AV) research. Recently, Autonomous Racing (AR) has become an area of research that attracts interest from multiple fields [1]. AR provides a suitable scenario for research in balancing performance and safety. On the one hand, racing provides agents with the apparent goal of getting ahead of other agents and clear punishments if an agent crashes. Top-tiered racing amplifies the outcome of strategically balancing different objectives. During Formula 1 championships from 1950 to 2022, the race winner achieved the fastest lap-time in only 40.2% of races [2]. The weak correlation between achieving the fastest lap times and winning is the empirical evidence that consistency and achieving the right balance between aggressiveness and restraint are crucial to success in the racing scenario. In this paper, we investigate the effect of weighing different objectives and propose a novel strategy for balancing these objectives for the ultimate goal to win the race.

A. Problem Setup

Our primary motivation is two-player racing games in close proximity. We begin by framing the multi-agent adversarial racing context as an *zero-sum extensive game* with *imperfect information* and *perfect recall*. Extensive games model sequential decision-making of players and naturally form a game tree where each node is a decision point for a player. The players get imperfect information since, at each

decision point, the other player’s action is unknown. The players also keep a history of all observable information. Thus they have perfect recall.

However, the planning problem presented in autonomous racing is continuous, and the state space of the agents, in turn, the game tree in the extensive game, will also be infinitely large if we model the game in the vehicle’s planning space. To make the game tractable, we define the notion of *Objective Space* \mathcal{O} . For each short rollout in an adversarial environment, we can compute multiple metrics regarding this agent’s performance, such as safety and aggressiveness. \mathcal{O} models the average outcome of each agent against competent opponents. Using \mathcal{O} , our planner maps complex agent behaviors to a lower dimension where only the episodic outcome is recorded instead of the entire decision-making process in the planning space. By nature, the mapping is surjective, i.e., a set of parameters for the agent planner can always be mapped to a single point in this space when using the same evaluation for each objective metric.

We define an action in our game as movements in a dimension of \mathcal{O} . This action space is analogous to the planning space in a grid world with actions that move the agent to a neighboring cell. Hence, we model our game-theoretic agents such that it plays the game in the \mathcal{O} . Two movements are available for each dimension: increasing or decreasing for a fixed distance along the axis. For example, four discrete actions are available at each turn when $\mathcal{O} \in \mathbb{R}^2$. Even with the formulation of agent action space, the possible objective values of an opponent agent or possible position in \mathcal{O} is still infinite. We propose a predictive model for regret values within Counterfactual Regret Minimization (CFR) [3] to make the problem tractable. Finally with head-to-head racing experiments, we demonstrate that using the proposed planning pipeline above significantly improves the win rate that generalizes to unseen opponents in an unseen environment.

B. Contributions

This work has four main contributions:

- 1) We propose a dimension reduction formulation that better discretizes an agent’s action space.
- 2) We display an efficient pipeline that optimizes agents’ parameters and constructs a Pareto front consisting of optimized agents across multiple objectives.
- 3) We propose an algorithm that predicts a racing agent’s counterfactual regret against different optimized agents.
- 4) Lastly, we provide a novel game-theoretic planning strategy that selects racing parameters using the prediction model.

All authors are with University of Pennsylvania, Department of Electrical and Systems Engineering, 19104, Philadelphia, PA, USA. Emails: {hongruiz, zhijunz, joebet, rahulm}@seas.upenn.edu

We organized the paper as follows: in Section II-A, we discuss agent parameterization and the implementation of the motion planner. In Section II-B, we discuss the evolution-based optimization for competent agent prototyping. In Section II-C, we discuss the CFR implementation and the prediction model training. In Section II-D, we present the online planning procedure of the game-theoretic planner. In Section III-B, we present the experimental results and discuss the implication of our hypotheses.

C. Related Work

Previous work has applied game-theoretic approaches to autonomous vehicles in adversarial scenarios or autonomous racing. Although there are game-theoretic approaches in autonomous driving, we do not make comparisons since, in racing, the driving scenarios are much less structured, and agent behaviors differ significantly from everyday driving. We focus our discussion of related work on comparing the advantages and disadvantages of this work to other work in the following aspects:

Game formulation: Differential games can model the dynamical system according to differential equations and are difficult to solve for non-linear dynamics. [4]–[6] formulate the game as a differential game. [7] formulate opponent identification as a multi-armed bandit problem. [8]–[15] all formulate racing as a general sequential game. The general form assumes little to no constraint on game states player actions. In comparison, we formulate the racing game as an extensive game with agent embeddings using the objective space. We traverse the game tree thoroughly to explore all outcomes of all agent actions during training.

Agent Action space formulation: The majority of the work in the space incorporates the game formulation directly into optimal control problems. These approaches require solving an optimization online to find actions, while ours choose the best action from a small number of possible actions. [4]–[6] use dynamic games; hence the action space for the agents is the same as the differential equations. [9]–[11] forms second-order piecewise polynomials with six coefficients as optimization variables to determine the car’s trajectory. [13] implements stochastic belief space dynamics using control inputs of the dynamic system where the agents’ actions. [14] implement an SQP incorporating the dynamical system and directly solve for control inputs. ALGAMES [15] also directly incorporates the dynamic system of the agents into an optimization problem.

Liniger et al. [8] formulate agents’ actions as selecting from a finite number of trajectories. This approach’s coverage of possible actions in the planning space heavily depends on granularity of control input discretization. Wrong parameters might lead to high computation times online.

Game solving and Nash equilibrium: To the authors’ knowledge, this is the first work to apply counterfactual regret minimization to racing games. By way of [3], [16], it was proven that Regret Matching (RM) with approximation converges to an ϵ -Nash equilibrium. Majority of the work [4]–[6], [9]–[11], [15] in this space use some

form of Best Response (BR). The convergence of BR is well studied. In most of these works, the planner aims to reach the Nash equilibrium in the best-case scenario. However, since racing is a real-time control task, equilibrium is not guaranteed at each planning step. [13] use iterative linear-quadratic Gaussian control (iLQG), and [14] forms an SQP to solve for control inputs and the equilibrium at the same time. These approaches form the optimization from the Nash equilibrium. Hence if the optimization converges, the equilibrium is reached simultaneously. ALGAMES [15] forms its unique class of game solver by using Lagrangian-augmented Newton’s method with convergence properties thoroughly studied.

Control strategies: Most of the work in this space uses some form of Model-predictive Control (MPC) as the control strategy since it is an optimal control problem, where the objective can be easily modified to include game information. [4]–[6], [13], [14] forms optimization problems to solve for control sequences. [9]–[11] solves for second-order polynomials as trajectories first, then use endogenous transformations to calculate the control sequences. [8] select control sequences by selecting a trajectory generated by discretized fixed input sequences. In comparison, we use a sampling-based scheme to select local goals for the car, then generate dynamically-feasible trajectories based on vehicle dynamics. After trajectory selection, the car follows the path via an adaptive Pure Pursuit tracker. This approach is widely popular because it’s easy to tune and highly efficient.

II. METHODOLOGY

We split the discussion of our approach into four sections: agent parameterization, offline Pareto front construction, offline training of the regret prediction model, and online game-theoretic objective space planning.

A. Motion Planner and Agent Parameterization

We use a sampling-based hierarchical motion planner similar to that of [17]. At the top level, the planner receives information on the current poses and velocities of the ego and the opponent, as well as an optimal race line generated using [18] for the current map. The race line consists of way-points as tuples of (x, y, θ, v) . Then n uniform grid points representing local goals are sampled around the race line (see Figure 1). Additionally, each goal point is assigned m scaling factors for the velocities on the corresponding trajectory. Then dynamically feasible trajectories are generated from the car’s current pose to the sampled goals using third-order clothoids combining methods from [19]–[23]. The velocity on each trajectory at each point is determined by scaling the velocity on the race line. Hence, the planner samples $n \times m$ trajectories at one planning step. The planner defines multiple cost functions to evaluate the quality of each trajectory for geometric properties and velocity profiles. We use the following cost functions: c_{mc} maximum curvature; c_{al} arc length of the trajectory; c_{hys} hysteresis loss that measures similarity to the previous selected trajectory; c_{do} distance to the optimal race line measured by lateral deviation; c_{co} collision with opponent based on differential speed to the

opponent at each time step; c_{v1} velocity cost that encourages higher speed; c_{v2} velocity cost that penalizes co-occurrence of high speed and high curvature.

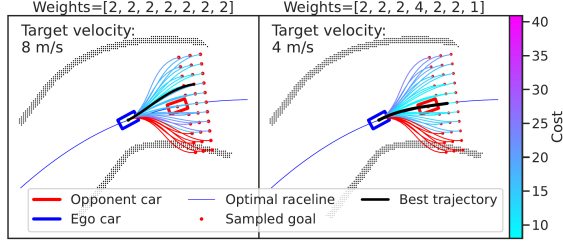


Fig. 1. Effect of the different weighting of cost functions on agent behavior. The red trajectories are in collision with the track, thus assigned infinite cost.

In addition, we include a global velocity scaling factor γ as another parameter for the agent to encourage convergence in agent optimization. Hence, each agent can be parameterized by the weight vector $w = [\gamma, p_{mc}, p_{al}, p_{phys}, p_{do}, p_{co}, p_{v1}, p_{v2}]$. Different w encodes different planning behavior thus we use it to define an agent. The planner calculates each sampled trajectory’s corresponding cost as the weighted sum of all costs $C = \sum_j p_j * c_j$. In addition, trajectories in collision with the environment are assigned infinite costs. The trajectory $k^* = \text{argmin}_{k \in [0, m * n]} C_k$ with the lowest total cost is then used as the selected trajectory at this planning step. Different cost weights lead to different planning behavior, as demonstrated in the scenario in Figure 1. As shown in the figure, the current longitudinal velocity of the opponent car is at 4.5 m/s. The cost weights on the left weigh the distance to the optimal race line less and collision with the opponent more. This disparity leads to the left agent selecting a trajectory deviating from the race line around the opponent vehicle while keeping higher velocities and the right agent selecting a trajectory that follows the opponent at a lower speed while still avoiding rear-ending the opponent. Finally, the planner uses Pure Pursuit [24] to track the selected trajectory.

B. Agent Optimization and Pareto Front Construction

Figure 2 shows the overall evolution-based optimization scheme. We will go over each component of the optimization in the following section.

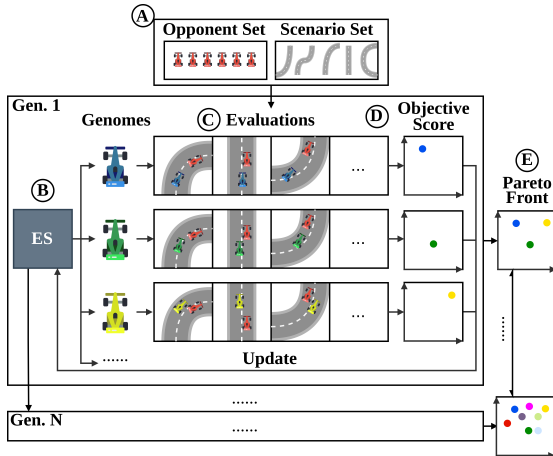


Fig. 2. Offline Agent Optimization and Pareto Front construction.

We first define the metrics we use as the dimensions of the objective space \mathcal{O} (Marker D in Figure 2). These are also the objective functions of agent multi-objective optimization. From the experiments, we found that designing the different dimensions as strictly competing encourages the exploration of diverse agents. Increasing the dimension of \mathcal{O} increases the number of possible actions at each step for the agents, increasing the game tree’s size. In theory, $|\mathcal{O}|$ is only limited by the computational budget in the self-play stage while collecting the training dataset for the prediction model training. The objective values are calculated episodically at the end of each consecutive short rollout in a race. In our experiments, the rollouts are 8 seconds long. We choose $\mathcal{O} \in \mathbb{R}^2$, $\mathcal{O} = [o_{agg}, o_{res}]$ in our racing case study and formulate them as follows: leftmargin=*

- Progress, or Aggressiveness: we use the difference between the progress of ego and opponent at the end of the rollout as the metric.

$$o_{agg} = S_e - S_o \quad (1)$$

where S is the curvilinear distance along the global race line.

- Safety, or Restraint: we use the instantaneous time to collision (iTTC) of the agent to calculate this metric:

$$o_{res} = a * \left(b - \frac{1}{T} \sum_{t \in T} \frac{r_t}{[r_t]_+} \right) \quad (2)$$

Where r is the range observation from the LiDAR. \hat{r} is the projections of the longitudinal velocity of the vehicle to the corresponding angles of the range rays. T is the number of individual range observations in the current episode. a is a scaling factor for the metric, and b is a constant. In our experiments, $a = 10$, $b = 5$.

In all the following experiments, the lower the value of o_{agg} , the more aggressive the agent; the lower the value of o_{res} , the more conservative the agent. We obtain the values of these metrics by running a simulated race lasting 8 seconds against an opponent.

Next, we define the Opponent set and Scenario set used for evaluation in the optimization (Marker A in Figure 2). We initialize the scenario set \mathcal{E} comprising a randomized relative position between the ego and an opponent on a randomized location on the race track. Each scenario is assigned an opponent with randomized agent parameters to create the opponent set \mathcal{P} . In our experiments, we use $|\mathcal{E}| = |\mathcal{P}| = 120$.

With these definitions, we now discuss the optimization implementation (Marker B in Figure 2). Use CMA-ES [25] as our evolutionary-based optimization algorithm. The optimization variable is the agent parameterization w , with o_{agg} and o_{res} as the objective functions. The ES samples multiple genomes of w with different values during each generation. Then each genomes is evaluated in a 8 second rollout in a batch against all opponent-scenario tuples $(\mathcal{P}, \mathcal{E})$. During every rollout, if the ego overtakes the opponent, the progress objective value o_{agg} is increased by 10%. If the ego crashes into the opponent, o_{agg} is increased by 10% and o_{res} is increased by 1. The final scores of the current genome

are the average objective scores over the entire batch with extra terms encouraging overtaking and penalizing crashing and are sent back to the ES. While optimizing, the objective values of each genome are stored to build the landscape of explored agents in the 2D objective space.

During the generations of the optimization, a Pareto front (Marker E in Figure 2) is maintained simultaneously. At the end of each generation, the top-performing genomes are kept in the Pareto front.

C. Regret Prediction Model

After obtaining the Pareto front \mathbb{P}_{pf} and the set of all explored agents \mathbb{P}_{all} from the ES, we create several different subsets of the explored agents using the objective space. First, we create a near-optimal set \mathbb{P}_{no} by taking all points in the explored agents within d_{near} away in Euclidean distance. Next, we use a Determinantal Point Process (DPP) [26] to sample N_{DPP} samples from the near-optimal set into \mathbb{P}_{DPP1} . In our experiments, we choose $d_{\text{near}} = 0.3$ and $N_{\text{DPP}} = 20$. We will use these subsets repeatedly during the next procedures. In the following section, we go over our game definition, counterfactual regret minimization (CFR) formulation, and creating the dataset for prediction model training.

Notation and Formal Game Model: We follow the convention in [3], [16] to define the formal game model. We denote the set of players as P , a node on the game tree, or history as $h \in H$. h is all current state information, including private information known to subsets of players. $Z \subseteq H$ denotes the set of terminal histories. Actions are denoted as $A(h) = a$ where h is non-terminal. Information set, or info set, $I_i \in \mathcal{I}_i$ for player i is similar to history but only contains information visible to player i . \mathcal{I}_i is the information partition for player i . $h \in I$ is the set of all histories that appear the same in the eye of the player. The strategy of player i is denoted as $\sigma_i \in \Sigma_i$, which is a distribution over actions $A(I_i)$, and Σ_i is the set of all strategies for player i . Moreover, strategy is the probability of taking action a given the information set I . σ is the strategy profile comprising all players' strategies. σ_{-i} is strategies of all players except i . The probability of reaching history h with strategy profile σ is denoted as $\pi^\sigma(h)$. And $\pi^\sigma(h)_{-i}$ denotes the probability of reaching h without player i 's contribution. The terminal utility, or payoff, of a player i for a terminal history $h \in Z$, is $u_i(h)$. History includes the opponent's record of actions while an info set does not. In our case, a history h includes the players' trajectories of positions in the objective space and the players' record of action taken at each step. The action space of each agent is increasing or decreasing a single objective value for a fixed amount d_{move} at a time. In all our experiments, we use $d_{\text{move}} = 1.0$. We define the terminal utility of the game as the lead S_{lead} of the winning agent on the curvilinear distance along the global race line. To keep the game zero-sum, the winning agent gets utility S_{lead} while the losing agent gets $-S_{\text{lead}}$.

Counterfactual Regret Minimization (CFR): regret is the utility a player did not get by not following the optimal strategy. We choose CFR due to its simplicity: during the

game, we simply choose the action with the best expected utility instead of solving an optimization online. The counterfactual value $v_i(\sigma, I)$ of player i is the expected utility of player i reaching I with probability of 1.

$$v_i^\sigma(I) = \sum_{z \in Z_I} \pi_{-i}^\sigma(z[I]) \pi^\sigma(z[I] \rightarrow z) u_i(z) \quad (3)$$

Where Z_I is the set of terminal histories reachable from I and $z[I]$ is the prefix of z up to I . $\pi^\sigma(z[I] \rightarrow z)$ is the probability of reaching z from $z[I]$. And $v_i^\sigma(I, a)$ follows the same calculation and assumes that player i takes action a at information set I with probability of 1. The immediate or instantaneous counterfactual regret is

$$r^t(I, a) = v_i^{\sigma^t}(I, a) - v_i^{\sigma^t}(I) \quad (4)$$

The *counterfactual regret* for information set I and action a on iteration T is

$$R^T(I, a) = \sum_{t=1}^T r^t(I, a) \quad (5)$$

Additionally, $R_+^T(I, a) = \max\{R^T(I, a), 0\}$, and $R^T(I) = \max_a \{R^T(I, a)\}$. Due to its simplicity, regret matching (RM) is typically used in CFR to pick the next action. In RM, the strategy for time $t + 1$ is:

$$\sigma^{t+1}(I, a) = \frac{R_+^t(I, a)}{\sum_{a' \in A(I)} R_+^t(I, a')} \quad (6)$$

If $\sum_{a' \in A(I)} R_+^t(I, a') = 0$, then any arbitrary strategy may be chosen. We choose the action with the highest counterfactual regret with probability one since it helps RM better cope with approximation errors [16].

Counterfactual Regret Prediction: Since calculating the counterfactual regret requires traversing the game tree, it becomes intractable when the number of possible information sets is infinite. Thus, we draw inspiration from value function approximation [27] in Reinforcement Learning and predict the counterfactual regret. The prediction model takes the current and history of the position of both the ego and the opponent in \mathcal{O} , the history of the ego's actions taken, and the candidate following action as the inputs and then predicts the counterfactual regret for the ego. Then the action with the highest counterfactual regret is chosen following Regret Matching.

D. Online Objective Space Planning

During the head-to-head race, we first obtain the pose and velocity of the opponent agent. We then simulate the current LiDAR scan of the opponent based on its current pose via ray marching. Over a short horizon (8 seconds in our case), we calculate the objective values of the opponent using the same formulation used in the offline optimization described in Section II-B. We pick an ego out of \mathbb{P}_{DPP1} and use its stored objective value and cost weights as the starting point of our ego planner. Once we reach the decision point for the ego planner, we encode the necessary information into the input for the prediction model. The ego then picks the action with the highest counterfactual regret value and takes the corresponding move in \mathcal{O} . The new operating point is selected by taking the nearest point in Euclidean distance

in \mathbb{P}_{no} and updating the planner cost weights accordingly. We keep iterating every 8 seconds until we reach a terminal state.

III. EXPERIMENTS

The goal of the experiments is to test two primary hypotheses: using the proposed game-theoretic planner significantly improves the win rate against competitive opponents; using the objective space to characterize agents with a lower dimension embedding is generalizable to different scenarios.

A. Simulation

We use a 2D racing simulator `fltenth_gym`¹ [28] with a single-track bicycle model with side slip [29]. In addition, the simulator includes 2D LiDAR simulations using ray-marching. The simulation is deterministic, and the physics engine can be explicitly stepped faster than real-time.

B. Experimental Results

We split our discussions on experiments into three parts: offline agent optimization, offline CFR prediction training, and online head-to-head racing. All code used for experiments can be found online².

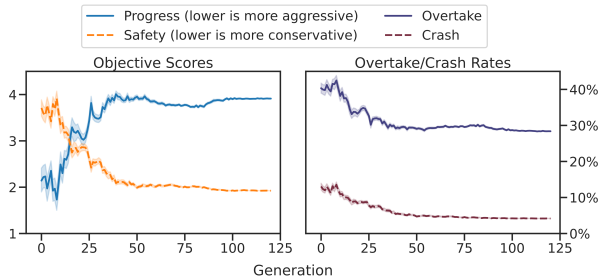


Fig. 3. ES optimization. x-axis denotes generations of 100 genomes.

Offline agent optimization: In our experiments, we choose CMA-ES [25] as our gradient-free optimization algorithm. We set up two competing optimization objectives in Aggressiveness and Restraint as described in Section II-B. The parameterization of each genome in the ES has seven cost weights ranging from 1.0 to 10.0 as described in Section II-A, and a velocity discount factor ranging from 0.6 to 1.0. The duration of each rollout is 8 seconds.

In Figure 3, we show the progression of the two competing objectives and crash and overtake rate during the optimization. The figure shows that the overtake rate is higher when the current parameterization is more aggressive. However, the crash rate is also higher. The trend of the objectives scores shows that the two objectives are competing, and we have explored a wide range of different parameterizations. Note that this optimization aims to explore a set of competitive prototype agents that are diverse in objective scores.

Figure 4 shows the subsets of prototypes \mathbb{P}_{all} , \mathbb{P}_{pf} , \mathbb{P}_{no} , and \mathbb{P}_{DPP1} in the 2D objective space using the procedure described in Section II-C. This figure shows the coverage of explored agents in the objective space.

Offline counterfactual regret prediction training: To construct the dataset for training of the prediction model,

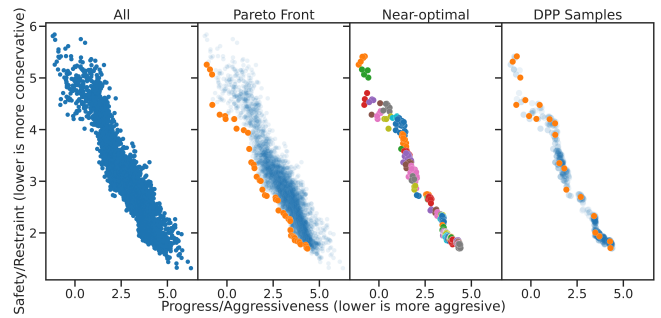


Fig. 4. Position of different sets of prototypes in the objective space.

we again use DPP to choose a subset \mathbb{P}_{DPP2} while ensuring $\mathbb{P}_{DPP1} \cap \mathbb{P}_{DPP2} = \emptyset$. For each pair in the Cartesian product $\mathbb{P}_{DPP1} \times \mathbb{P}_{DPP2}$, there exists a unique game tree where each branch is a unique combination of possible actions for both players. We play games between each member of the product set until the game reaches a terminal state. In our experiments, each agent is allowed three moves in total, and 4 possible actions at each decision point. Thus, the number of branches for each player’s game tree is $4^3 = 64$. Then we play out the games between each combination of possible action sequences of the ego and the opponent, resulting in $64^2 = 4096$ games. With $N_{DPP} = 20$, we will then in total play $20^2 * 4096 = 1638400$ 32 second rollouts. At the end of each game, we store the utility for each corresponding game for query later. Afterward, we traverse the game tree for the ego agent to calculate the counterfactual regret. At each node of the ego’s game tree, we treat playing against the opponent using one possible action sequence out of all possible sequences as an iteration in CFR and calculate the counterfactual regret for the current node following Equation 5. A dataset of tuples (I, a, R) is built during this stage. Each infostet I consists of the current history of ego agent objective values, history of opponent agent objective values, masks of ego and opponent objective values, and ego agent history of actions. We encode objective values to fixed-length vectors with zero padding. Masks are set up such that only positions with objective values are filled with ones; otherwise, zeros. All actions are one-hot encoded. In total, the input feature size for the prediction model is 40. We use a multi-layer perceptron (MLP) with one hidden layer of size 2048 and leaky ReLU activation between layers. We train the network with L1 loss, batch size of 1024, and Adam optimizer with adaptive learning rate (starting at 0.005, reduce when validation loss plateaus for ten steps) in 2000 epochs.

Simulated Racing: We record the win rate of our approach against different opponents on different maps. We designate the ego agent as the winner if its progress along the global race line is more than that of the opponent at the end of the game. To ensure fairness, the agents start side by side at the same starting line on the track and alternate starting positions. The starting positions are also randomized five times while ensuring agents are side by side. To show the effect of the planner being game theoretic, we report results of paired t-tests against all opponents (with a null hypothesis that being game-theoretic does not change the win rate). The non game-theoretic opponents is selected from

¹https://github.com/fltenth/fltenth_gym

²https://github.com/hzheng40/objective_space_cfr

\mathbb{P}_{DPP2} . Instead of making a move at every step, the cost weights of these opponents stay constant. To demonstrate the effect of the agent optimization, we play against random explored opponents using the same planner with constant cost weights from $\mathbb{P}_{all} \setminus \mathbb{P}_{no}$. To show that the mapping from planning space to objective space is an effective way of characterizing agents, we play against a competitive planner unseen (winning strategy lane switcher from the FITENTH ICRA 2022 Race [30]) during training. The lane switcher creates multiple lanes around the race track. By default, it follows an optimal race line around the track. Once the agent encounters an obstacle, it switches to an unoccupied lane and tracks it with Pure Pursuit. Lastly, we perform all experiments described on an unseen map during training to show that correct objective value designs are agnostic of the evaluation environment. The ego agent starts with a sample within \mathbb{P}_{DPP1} . The non-game-theoretic ego does not predict CFR and changes cost weights, and the game-theoretic ego uses our entire online pipeline. We summarize the results of the online experiments in Table I. Each table cell consists of statistics from data points from $20^2 * 2 * 5 = 4000$ games.

TABLE I

WIN-RATES IN HEAD-TO-HEAD RACING EXPERIMENTS WITH P-VALUES.

Opponent	Ego		p-value
	Win-rate Non game-theoretic	Win-rate Game-theoretic	
On Seen Map			
Non game-theoretic	0.515 ± 0.251	0.569 ± 0.213	0.0142
Random explored	0.624 ± 0.225	0.670 ± 0.199	0.00370
Unseen	0.586 ± 0.101	0.597 ± 0.089	0.0863
On Unseen Map			
Non game-theoretic	0.553 ± 0.256	0.628 ± 0.180	0.0124
Random explored	0.625 ± 0.278	0.738 ± 0.172	0.00276
Unseen	0.556 ± 0.101	0.565 ± 0.098	0.147

Effect of being game-theoretic: The main result of our experiment is that the p-value is small enough to reject the null hypothesis that being game-theoretic does not change the win rate. Turning on the game-theoretic pipeline and changing the cost weights dynamically significantly increases the win rate. Although not as significant when playing an unseen opponent, the trend is still clearly shown. This finding validates our prediction model and the effect of CFR by showing significant improvement.

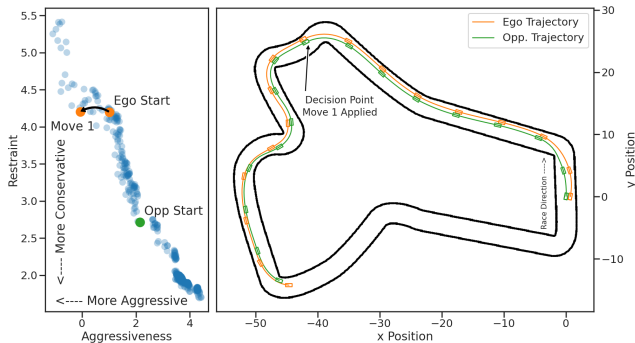


Fig. 5. Effect of making a move in \mathcal{O} in motion planning space.

Agent characterization with the objective space: Another hypothesis of this paper is that creating agent embeddings using the objective space models agent behavior

and helps with generalization. In Figure 5, we examine two episodes of rollouts in one of the races played in the head-to-head experiment. In the first segment (before the decision point), the ego uses the starting cost weights to plan and observe the opponent for 8 seconds. The prediction model tells the planner to increase aggressiveness (left subplot) at the decision point. The planner switches to the new cost weights corresponding to the new position in the objective space. The effect of the move is evident since the ego slowed down less than the opponent in the second segment (after the decision point) in the chicane and overtook the opponent by the end of the second episode.

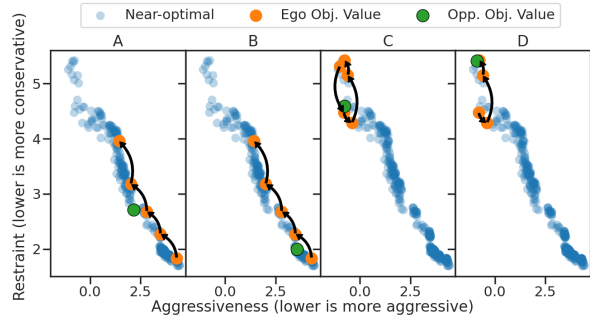


Fig. 6. Trajectories of ego moves in \mathcal{O} .

The results also validate this hypothesis by showing the improvement transfers to unseen agents in unseen environments. In Figure 6, we investigate the interaction dynamics between ego agents winning against competitive opponent agents. In sub-figures A and B, the opponent agent is embedded into the lower right quadrant of the objective space, meaning that these agents value safety more than progress. In these scenarios, the ego agent, starting from the lower right quadrant, became more aggressive than conservative in all moves. In sub-figures C and D, the opponent agent is embedded into the upper left quadrant of the objective space, meaning that these agents value progress more than safety. On the contrary, in these scenarios, the ego decides to make early moves to increase restraint and, later on, increase aggressiveness.

IV. CONCLUSION

We could potentially improve our methodology and experimental design to strengthen the findings. First, the planner could implement a receding horizon scheme when playing the extensive game. Second, experiments should investigate bias in evaluation scenarios during the race to hopefully eliminate the effect of randomness when selecting prototypes using DPPs. The central hypotheses of this paper are that using the proposed game-theoretic planner using agent characterization with the objective space significantly improves the win rate against different opponents, and the improvement is transferable to unseen opponents in an unseen environment. We first define the objective space, then perform agent optimization via CMA-ES. Next, we train a regret prediction model and implement an online planning pipeline that uses CFR to maximize the win rate. Lastly, we provide statistical evidence that shows significant improvements to the win rate that generalizes using the proposed game-theoretic planning strategy.

REFERENCES

- [1] J. Betz, H. Zheng, A. Liniger, U. Rosolia, P. Karle, M. Behl, V. Krovi, and R. Mangharam, "Autonomous Vehicles on the Edge: A Survey on Autonomous Vehicle Racing," *IEEE Open Journal of Intelligent Transportation Systems*, vol. 3, pp. 458–488, 2022, conference Name: IEEE Open Journal of Intelligent Transportation Systems.
- [2] "Formula 1 World Championship (1950 - 2022)." [Online]. Available: <https://www.kaggle.com/datasets/rohanrao/formula-1-world-championship-1950-2020>
- [3] M. Zinkevich, M. Johanson, M. Bowling, and C. Piccione, "Regret Minimization in Games with Incomplete Information," in *Advances in Neural Information Processing Systems*, vol. 20. Curran Associates, Inc., 2007. [Online]. Available: <https://proceedings.neurips.cc/paper/2007/hash/08d98638c6fcd194a4b1e6992063e944-Abstract.html>
- [4] R. Spica, E. Cristofalo, Z. Wang, E. Montijano, and M. Schwager, "A real-time game theoretic planner for autonomous two-player drone racing," *IEEE Transactions on Robotics*, vol. 36, no. 5, pp. 1389–1403, 2020.
- [5] G. Williams, B. Goldfain, P. Drews, J. M. Rehg, and E. A. Theodorou, "Autonomous racing with autorally vehicles and differential games," 2017.
- [6] —, "Best response model predictive control for agile interactions between autonomous ground vehicles," in *2018 IEEE International Conference on Robotics and Automation (ICRA)*. IEEE, May 2018. [Online]. Available: <https://doi.org/10.1109/icra.2018.8462831>
- [7] A. Sinha, M. O'Kelly, H. Zheng, R. Mangharam, J. Duchi, and R. Tedrake, "Formulazero: Distributionally robust online adaptation via offline population synthesis," in *International Conference on Machine Learning*. PMLR, 2020, pp. 8992–9004.
- [8] A. Liniger and J. Lygeros, "A noncooperative game approach to autonomous racing," *IEEE Transactions on Control Systems Technology*, vol. 28, no. 3, pp. 884–897, 2019.
- [9] M. Wang, Z. Wang, J. Talbot, J. C. Gerdes, and M. Schwager, "Game theoretic planning for self-driving cars in competitive scenarios," in *Robotics: Science and Systems XV, University of Freiburg, Freiburg im Breisgau, Germany, June 22-26, 2019*, A. Bicchi, H. Kress-Gazit, and S. Hutchinson, Eds., 2019. [Online]. Available: <https://doi.org/10.15607/RSS.2019.XV.048>
- [10] Z. Wang, R. Spica, and M. Schwager, "Game Theoretic Motion Planning for Multi-robot Racing," in *Distributed Autonomous Robotic Systems*, vol. 9. Springer, 2020, pp. 225–238. [Online]. Available: http://link.springer.com/10.1007/978-3-030-05816-6_16
- [11] G. Notomista, M. Wang, M. Schwager, and M. Egerstedt, "Enhancing game-theoretic autonomous car racing using control barrier functions," in *2020 IEEE International Conference on Robotics and Automation (ICRA)*. IEEE, May 2020. [Online]. Available: <https://doi.org/10.1109/icra40945.2020.9196757>
- [12] C. Jung, S. Lee, H. Seong, A. Finazzi, and D. H. Shim, "Game-theoretic model predictive control with data-driven identification of vehicle model for head-to-head autonomous racing," *arXiv preprint arXiv:2106.04094*, 2021.
- [13] W. Schwarting, A. Pierson, S. Karaman, and D. Rus, "Stochastic dynamic games in belief space," *IEEE Transactions on Robotics*, pp. 1–16, 2021. [Online]. Available: <https://doi.org/10.1109/tro.2021.3075376>
- [14] E. L. Zhu and F. Borrelli, "A sequential quadratic programming approach to the solution of open-loop generalized nash equilibria," 2022.
- [15] S. Le Cleac'h, M. Schwager, and Z. Manchester, "ALGAMES: a fast augmented lagrangian solver for constrained dynamic games," *Auton. Robots*, vol. 46, no. 1, pp. 201–215, Jan. 2022.
- [16] N. Brown, A. Lerer, S. Gross, and T. Sandholm, "Deep Counterfactual Regret Minimization," Nov. 2018. [Online]. Available: <https://arxiv.org/abs/1811.00164v3>
- [17] D. Ferguson, T. M. Howard, and M. Likhachev, "Motion planning in urban environments," *Journal of Field Robotics*, vol. 25, no. 11-12, pp. 939–960, 2008, publisher: Wiley Online Library.
- [18] A. Heilmeyer, A. Wischniewski, L. Hermansdorfer, J. Betz, M. Lienkamp, and B. Lohmann, "Minimum curvature trajectory planning and control for an autonomous race car," *Vehicle System Dynamics*, 2019, publisher: Taylor & Francis.
- [19] B. Nagy and A. Kelly, "Trajectory generation for car-like robots using cubic curvature polynomials," *Field and Service Robots*, vol. 11, pp. 479–490, 2001.
- [20] A. Kelly and B. Nagy, "Reactive nonholonomic trajectory generation via parametric optimal control," *The International Journal of Robotics Research*, vol. 22, no. 7-8, pp. 583–601, 2003.
- [21] T. M. Howard and A. Kelly, "Optimal rough terrain trajectory generation for wheeled mobile robots," *The International Journal of Robotics Research*, vol. 26, no. 2, pp. 141–166, 2007.
- [22] T. M. Howard *et al.*, "Adaptive model-predictive motion planning for navigation in complex environments," 2009.
- [23] M. McNaughton, C. Urmson, J. M. Dolan, and J.-W. Lee, "Motion planning for autonomous driving with a conformal spatiotemporal lattice," in *2011 IEEE International Conference on Robotics and Automation*. IEEE, 2011, pp. 4889–4895.
- [24] R. C. Coulter, "Implementation of the pure pursuit path tracking algorithm," Carnegie-Mellon UNIV Pittsburgh PA Robotics INST, Tech. Rep., 1992.
- [25] N. Hansen, "The CMA evolution strategy: A tutorial," *arXiv preprint arXiv:1604.00772*, 2016.
- [26] A. Kulesza and B. Taskar, "Determinantal point processes for machine learning," *Foundations and Trends® in Machine Learning*, vol. 5, no. 2-3, pp. 123–286, 2012, arXiv:1207.6083 [cs, stat]. [Online]. Available: <http://arxiv.org/abs/1207.6083>
- [27] R. S. Sutton and A. G. Barto, *Reinforcement learning: An introduction*. MIT press, 2018.
- [28] M. O'Kelly, H. Zheng, D. Karthik, and R. Mangharam, "FITENTH: An Open-source Evaluation Environment for Continuous Control and Reinforcement Learning," in *NeurIPS 2019 Competition and Demonstration Track*. PMLR, 2020, pp. 77–89.
- [29] M. Althoff, M. Koschi, and S. Manziinger, "CommonRoad: Composable benchmarks for motion planning on roads," in *2017 IEEE Intelligent Vehicles Symposium (IV)*. IEEE, 2017, pp. 719–726.
- [30] "Fitenth icra 2022: Results." [Online]. Available: <https://icra2022-race.fitenth.org/results.html>